PCCP

Accepted Manuscript

This article can be cited before page numbers have been issued, to do this please use: L. Mena, M. D. A. Vera, M. T. Baumgartner and L. Jimenez, *Phys. Chem. Chem. Phys.*, 2019, DOI: 10.1039/C9CP02028D.

ROYAL SOCIETY OF CHEMISTRY

rsc.li/pccp

View Article Online
DOI: 10.1039/C9CP02028D

ARTICLE

Adiabatic deprotonation as an important competing pathway to ESIPT in photoacidic 2-phenylphenols

Received 00th January 20xx,
Accepted 00th January 20xx

DOI: 10.1039/x0xx00000x

Leandro D. Mena,*[a] D. M. A. Vera,[b] Maria T. Baumgartner[a] and Liliana B. Jimenez*[a]

ESIPT (Excited State Intramolecular Proton Transfer) to C atom in 2-phenylphenol is known to occur as an intrinsically inefficient process; however, to the best of our knowledge, a structure-ESIPT efficiency relationship has not been elucidated yet. Here we show that there exists a competitive interplay between photoacidity and ESIPT efficiency for 2-phenylphenol system. The attachment of electron withdrawing groups to the phenol moiety promotes adiabatic deprotonation in excited state and diminish the charge transfer character of excitations, both factors contributing to decrease the ESIPT reaction yield. On the other hand, unfavorable conformational distribution in ground state also appears as another important aspect responsible for the low ESIPT extent of 2-phenylphenol. A new derivative bearing electron donor, bulky substituents at ortho and para positions of the phenol ring shows an outstanding ESIPT performance, which demonstrates that the efficiency of the process can be significatively enhanced by modifying the substitution pattern. We anticipate our results will help guide molecular design to produce new compounds with high ESIPT efficiency.

Introduction

Photoacids are organic light-absorbing molecules that present an exacerbated tendency to act as proton donors upon photoexcitation, becoming more acidic in excited state than in ground state.[1] This acidity enhancement results in a large pK_a drop, thus excited-state pK_a (pK_a*) can reach slightly greater than zero values in the case of "normal" photoacids, or even negative values for the so-called "super" photoacids.[2] By far, hydroxyarenes (phenols, naphthols, hydroxypyrenes, among others) are the most studied group of photoacidic compounds.[3] One of the most prominent examples is 1-naphthol, whose pK_a* is 0.4, considerably smaller than its ground-state pKa of 9.2.[4] Because of this peculiar behaviour and its potential applications, hydroxyarene photoacids have attracted much attention in last decades.[5] Photoinduced dissociation of hydroxyarenes in solution phase generally occurs as an intermolecular event known as Excited State Proton Transfer (ESPT),[6] in which a solvent molecule (or any basic molecule) can act as the proton acceptor. Naturally, most studies dealing with photoacids have been conducted in water,[7] although a few reports regarding superphotoacids with ability to experience ESPT in nonaqueous environments can be found in literature.[8] Moreover, it must be recalled that many of these processes take place on an ultrafast time scale, making its experimental study a challenging task.[9] In molecules having both proton donor and acceptor in close proximity the excited state proton transfer can proceed through an intramolecular mechanism termed ESIPT, besides the aforementioned intermolecular process (Scheme 1).[9] As with acidity, basicity also increases in excited state; thus, a group presenting poor ground-state basicity can easily accept a proton once the molecule has been excited.[10] A good example of this is ESIPT to sp^2 or sp hybridized carbon atoms, in which a C atom (weakly basic in S_0) becomes able to receive a proton in excited state.[11] This case is quite peculiar, since

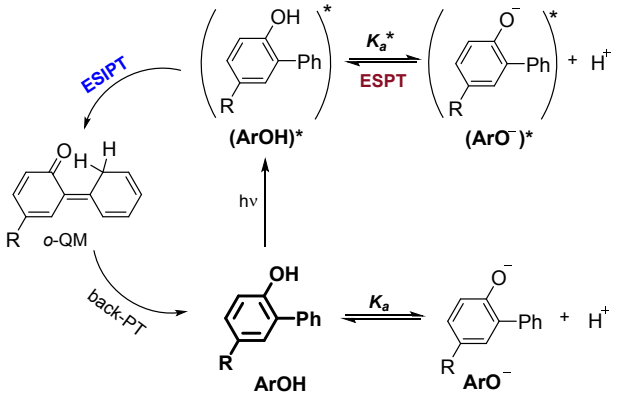

Scheme 1. ESPT and ESIPT processes of *p*-substituted 2-phenylphenols.

[a] INFIQC, Departamento de Química Orgánica
Facultad de Ciencias Químicas, Universidad Nacional de Córdoba
Ciudad Universitaria, Córdoba, Argentina
E-mail: lmena@fcq.unc.edu.ar, ljimenez@fcq.unc.edu.ar
[b] QUIAMM-INBIOTEC- Departamento de Química
Facultad de Ciencias Exactas y Naturales, Universidad Nacional de Mar del Plata
Mar del Plata, Argentina

† Footnotes relating to the title and/or authors should appear here.
Electronic Supplementary Information (ESI) available: [details of any supplementary information available should be included here]. See DOI: 10.1039/x0xx00000x

most ESIPT processes usually involve carbonylic oxygen or heterocyclic nitrogen atoms as the basic sites.[12]

In their seminal work,[13] Lukeman and Wan described ESIPT in 2-phenylphenol, where the hydroxylic proton of phenol is transferred to an aromatic carbon atom at the *ortho* position of the adjacent phenyl ring, to give an *ortho* quinone methide (*o*-QM). Since then, many similar systems were reported, in which ESIPT occurs together with other processes such as water-mediated intramolecular proton transfer to distal sites on the same molecule or proton transfer to bulk solvent.[14] However, the connection between photoacidity and ESIPT reactivity in those systems remains scarcely explored yet. Unlike other examples in which an increase of the photoacidity leads to barrierless, exergonic ESIPT,[15] the case of 2-phenylphenol seems to be substantially different. A quantum yield of deuterium incorporation (an indirect measure of ESIPT efficiency) of 0.041 for 2-phenylphenol suggests that a competition with other more efficient pathways is highly possible. To confirm this assumption, we explored the relationship between ESPT and ESIPT in a new family of photoacidic 2-phenylphenols, and at the same time we were able to obtain "normal" to "super" photoacids through simple molecular modifications. This paper presents the detrimental effect on ESIPT performance induced by increasing the photoacidity of 2-phenylphenol derivatives and clarifies the role of ESPT as a competing photochemical pathway.

Results and Discussion

2-Phenylphenol derivatives **1-5** were obtained from Suzuki-Miyaura cross-coupling reactions in moderate to good yields and purified by column chromatography. The introduction of R groups was carried out exclusively at *para* position of phenol moiety, in order to facilitate the analysis of substituent electronic effect. The indirect detection of ESIPT in **1-5** was performed by monitoring the regiospecific incorporation of deuterium upon irradiation in a protic solvent, according to the method reported by Wan and co-workers (Scheme 2).[16] As ESIPT to carbon atoms is a process that occurs within femtoseconds, Wan *et al.* designed an alternative, simple methodology for ESIPT detection that consists in performing the irradiation of the compounds in a protic deuterated solvent. In such an environment, the exchange of hydroxylic proton by deuteron takes place; then, upon photoexcitation, the deuteron is transferred to the adjacent phenyl ring to give the *keto* tautomer. After relaxation and back-tautomerization, the starting material is recovered isotopically labelled at the

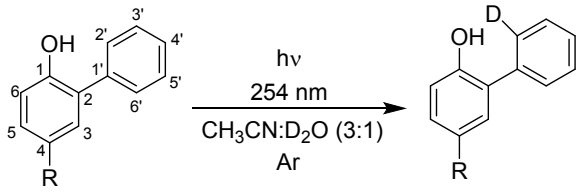

R= H (**1**), OMe (**2**), *t*-Bu(**3**), COOMe (**4**), CN (**5**)

phenyl ring; following the deuterium incorporation by ^{1}H NMR and MS, the ESIPT reaction extent can be estimated. By performing the irradiation of a solution of **1** in a 3:1 CH_3CN/D_2O mixture with 254 nm light for 1 h we obtained a 40% D-incorporation at the *ortho* position of the adjacent phenyl ring.[17] In this work we are focusing only in intrinsic ESIPT to the *ortho* position of the phenyl ring, without addressing for water- mediated proton transfer to distal sites

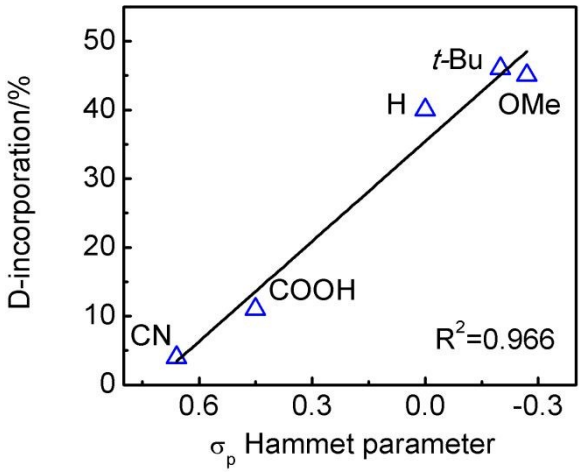

Fig. 1 Plot of D-incorporation percentage vs. σ_p Hammett parameter for compounds 1-5.

Table 1. Deuterium incorporation in the photolysis of compounds **1-5**[a]

Compound	D-incorporation
1	40
2	45
3	46
4[b]	11
5	4

[a] Percentage deuterium exchange at the 2' position of 2-phenylphenol derivatives following photolysis in a 3:1 CH_3CN/D_2O mixture, measured by ^{1}H NMR (400 MHz). [b] To avoid photodegradation of compound **4**, the carboxylic acid derivative was employed instead.

(i.e. 4´ position). In Table 1 the results of photolyses of derivatives **1-5** are displayed. As can be seen, the ESIPT reaction yield decreases as the electron withdrawing character of substituent R rises, becoming almost negligible when R=CN. A plot of D-incorporation extent vs. the σ_p Hammett parameter shows a straight linear correlation, indicating the existence of a close relationship between the nature of R substituent and the ESIPT performance (Figure 1).

It is well-known that acidity (and, simbatically, photoacidity) of phenols can be modulated by incorporating electron withdrawing/donating substituents on the *ortho* and *para* ring positions, [18] which allows pK_a and pK_a* to be finely tuned. An enhancement in photoacidity implies that the proton can be released more easily, but this does not necessarily result in a higher ESIPT performance. To quantify both acidity/photoacidity in our 2-phenylphenol series, aqueous pK_a

Scheme 2 Photochemical reaction of *p*-substituted 2-phenylphenols

View Article Online
DOI: 10.1039/C9CP02038D

and pK_a* values for **1, 2, 4** and **5** were determined (**3** derivative was excluded because of its poor solubility in water). Ground-state pK_a measurement was carried out using UV-Vis spectrophotometry, recording the absorption spectra for each compound in a pH range of 4-13. The pK_a* determination was performed employing the Förster cycle (Eq. 1, see ESI for spectroscopic details). [19]

$$\Delta pKa^* = pKa - pKa^* = \frac{0.625\ (\nu ArOH - \nu ArO^-)}{T}$$

Table 2. Experimental pK_a and pK_a* values for 2-phenylphenol derivatives (**1-5**) and literature values for *p*-substituted phenol analogues (without phenyl ring).

R	2-phenylphenol series		Phenol series	
	pK_a	pK_a*	pK_a [a]	pK_a*[b]
H (**1**)	10.04±0.03	1.59± 0.09	9.99	4.0
OMe (**2**)	10.36± 0.04	2.96± 0.03	10.27	5.6
t-Bu (**3**)	-	-	10.30	-
COOMe (**4**)	8.13± 0.06	-1.57± 0.03	8.47	-
CN (**5**)	7.88± 0.03	-1.62± 0.03	7.96	3.3

[a] Ref. 20. [b] Ref. 1.

In Table 2 the obtained pK_a and pK_a* values for each compound are presented. As expected, both ground and excited state acidities rise with the attaching of electron withdrawing groups (EWG) to the molecule. pK_a* values go from 2.96 to -1.62, indicating that the series include normal (**1** and **2**) and superphotoacids (**4** and **5**). *t*-Butyl-containing derivative **3** is expected to act as a normal photoacid (*vide infra*). The obtained pK_a* of 1.59 for **1** agrees with the estimated 1.15 reported in literature. [16]

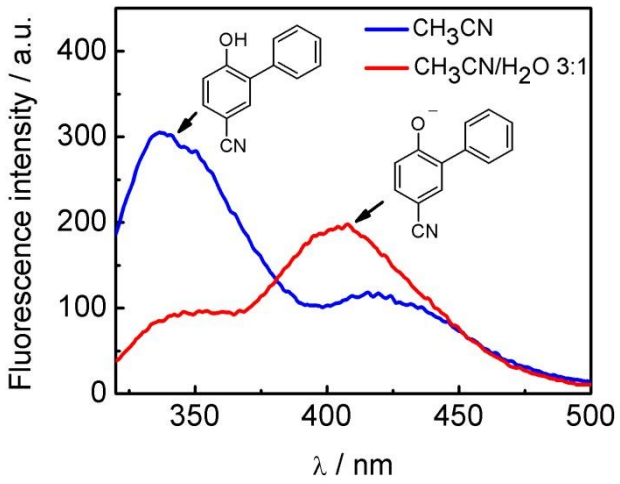

Fig. 2 Fluorescence emission spectra of p-CN-2-phenylphenol (**5**) in CH3CN and in a CH_3CN:H_2O (3:1) mixture as solvents. The emission band at 419 nm in neat CH_3CN is assigned to the deprotonated form (**5**$^-$).

Interestingly, pK_a's remain almost unchanged if compared with the corresponding values from the phenol series (without the phenyl ring, Table 2),[20] but it can be noted that 2-phenylphenols are more acidic in S_1 state than their simpler analogues. This may be due to the strong OH$\cdots\pi$ interaction that 2-phenylphenols present in excited state, which weaken the O-H bond; the existence of this interaction is known to be a prerequisite for ESIPT to occur.

ESIPT in **1** can be enhanced by shifting the acid-base equilibrium towards the undissociated form of 2-phenylphenol, as can be deduced from the 50% of D-incorporation obtained from the photolysis of **1** in a 3:1 CH_3CN/D_2O mixture at pH(D) 1 (adjusted with concentrated DCl). When the same experiment was performed for **5**, no change in the D-exchange yield with respect to the experiment conducted at pH(D) 7 was observed, suggesting that **5** possess a pK_a* lower than 1, which is consistent with the measured pK_a* of -1.62. Furthermore, steady state fluorescence measurements are in accordance with the observed trend. The spectrum of **1** in CH_3CN revealed a single emission band corresponding to the phenol form, whereas in the 3:1 CH_3CN/H_2O mixture a shoulder at 420 nm was detected as the characteristic emission of the phenolate anion formed by an adiabatic proton transfer to the solvent (SI 3.4). [16] On the other hand, emission spectra of **5** confirms the presence of the anion even in neat CH_3CN, which illustrate the character of **5** as a superphotoacid. In the CH_3CN/D_2O mixture the amount of anion is greater, as seen in the emission spectrum (Figure 2).

Time-resolved fluorescence spectroscopy was then used to characterize the lifetime of the undeprotonated and deprotonated species for each compound (**1-5**, Table 3). Fluorescence lifetimes in water decrease as the electron withdrawing character of the substituents rise for both undeprotonated and deprotonated species, which could be related to electron effects of EWG groups. Nevertheless, this trend is more marked for undeprotonated species, which can also be related -at least partially- to the fact that ESPT to solvent (a relevant deactivating pathway from S_1) is favoured for EWG-substituted compounds.[16]

Table 3. Fluorescence lifetimes of undeprotonated (AH) and deprotonated (A^-) forms of compounds **1**, **2** and **5** in water.[a]

Compound	τ (AH)/ns (λ_{em} / nm)	τ (A^-) /ns (λ_{em} / nm)
1	0.256 ± 0.003 (348)	3.722 ± 0.006 (414)
2	1.881 ± 0.006 (384)	5.079 ± 0.009 (455)
5	0.102 ± 0.005 (335)	1.07 ± 0.04 (395)

[a] Fluorescence lifetimes of aerated solutions measured at pH 1 (AH) and at pH 13 (A^-). λ_{exc} = 267 nm.

TD-DFT calculations were performed to gain a deeper insight into the ESIPT performance of the 2-phenylphenol series. Although previous computational studies involved mostly multi-reference calculation methods,[21] it has been demonstrated that TD-DFT (a less computationally expensive

Table 4. Theoretically predicted pK_a and pK_a*.[a]

Compound	pK_a	pK_a*
1	9.59 (0.45)	2.07 (-0.48)
2	9.18 (1.18)	2.74 (0.22)
3	9.68 (-)	2.22 (-)
4	6.50 (1.63)	-1.51 (-0.05)
5	5.85 (2.03)	-1.73 (0.11)

[a] Difference with respect to experimental values are given in parentheses, as p$K_{a\text{Exp}}$ (pK_a*$_{\text{Exp}}$) - p$K_{a\text{Theo}}$ (pK_a*$_{\text{Theo}}$). See ESI for more details.

method) gives quite reliable results for the proton transfer process in the ππ* state, despite the single-reference character of the method.[22] Our theoretically predicted pK_a and pK_a* values agree well with our experimental results and confirm that photoacidity can be strongly affected by the substitution pattern (Table 4). An MSE (mean signed error with respect to the experimental values) of 1.32 units illustrates the accuracy of the employed method for the pK_a computation. Theoretical calculation of pK_a* was achieved using the Förster cycle in the same manner as in the experimental work. The agreement with experimental data is excellent, with an MSE value of -0.04. Since the Förster cycle requires the determination of absorption and emission maxima wavelengths, the success of the theoretical prediction relies on the quality of the chosen method to reproduce the experimental spectroscopic information. In this regard, the use of a long-range corrected functional such as CAM-B3LYP for the computation of vertical absorption and emission energies was expected to be the most reliable approach, considering the possibility of a marked charge transfer character for most electron donor substituted species (see below).

The molecular modeling of ESIPT process was performed at TD-DFT CAM-B3LYP/6-31+G(d) level of theory, in acetonitrile.

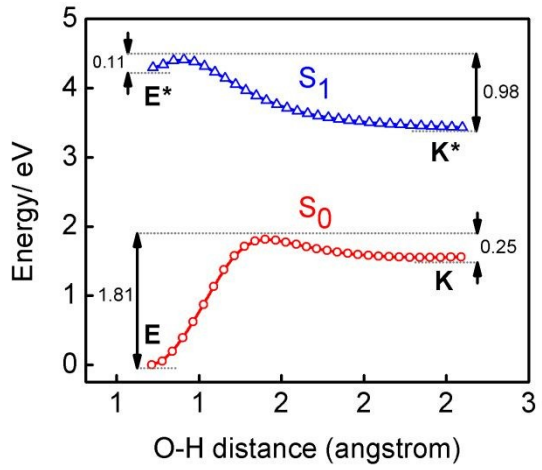

Fig. 3 Potential energy curves of the S_0 and S_1 states of 1 in acetonitrile obtained from relaxed scans along the OH stretching coordinate (step length=0.05 Å). Proton transfer energy barriers and ΔE for the keto form with respect to TS are indicated.

For the sake of comparison, only compounds **1**, **2** and **5** were studied. Energies of *enol*/*keto* minima in both S_0 and S_1 states, vertical absorption energies and main geometric parameters are presented in Table 5. Despite CAM-B3LYP slightly overestimates the vertical absorption energies for **1** and **2**, the charge transfer character of the overall process makes necessary the use of a long-range corrected functional.

In Fig. 3 the potential energy surfaces (PES) in both ground and first singlet states of **1** are shown. The *enol* minimum in S_1 lies 0.64 eV below vertical excitation (Table 5), in accordance with Xia *et al.* results.[21a] The dihedral angle between the two rings is reduced from 58.2° in S_0 to 21.5° in the S_1 state, resulting in a shortening of $C_{acceptor}$-H bond distance from 2.44 Å (S_0) to 2.16 Å (S_1). These geometrical changes lead to a stronger OH···π interaction in S_1 state, as was stated elsewhere.[16] NCI

Table 5. Selected geometric and energetic parameters for compounds **1**, **2** and **5** computed at CAM-B3LYP/6-31+G(d) level in acetonitrile.

	Compound					
	1 (H)		**2 (OMe)**		**5 (CN)**	
Geometric parameters	S_0	S_1	S_0	S_1	S_0	S_1
C1-C2-C1'-C2' angle *enol*	58.2	21.5	57.3	29.4	59.2	19.4
C1-C2-C1'-C2' angle *keto*	0.0	82.6	0.1	84.3	0.0	74.2
$O_{22}H_{23}$ distance (Å) *enol* [a]	0.97	0.98	0.97	0.98	0.97	0.98
$C_{12}H_{23}$ distance (Å) *enol* [b]	2.44	2.16	2.44	2.13	2.44	2.24
Energetic parameters	S_0	S_1	S_0	S_1	S_0	S_1
Relative energy *enol* (eV) [c]	0.00	4.29	0.00	4.07	0.00	4.36
Relative energy *keto* (eV) [c]	1.55	3.43	1.61	3.17	1.53	3.58
Vertical excitation (eV)	4.94		4.52		4.94	
K* relaxation energy (eV) [d]	0.80 (0.0018)		0.38 (0.0005)		1.28 (0.019)	

[a] O_{22} and H_{23} are the atoms forming the phenolic OH, according to G09 input numbering. [b] C_{12}=carbon atom acceptor. [c] Calculated energies relative to the *enol* form in ground state for each compound. [d] Relaxation energies of *keto* excited species, with oscillator strength in parentheses.

(non-covalent interactions) analysis (SI 4.3.3) results show the existence of a non-covalent interaction between the phenolic OH and the π system in S_0 that becomes stronger in the S_1

View Article Online
DOI: 10.1039/C9CP02028D

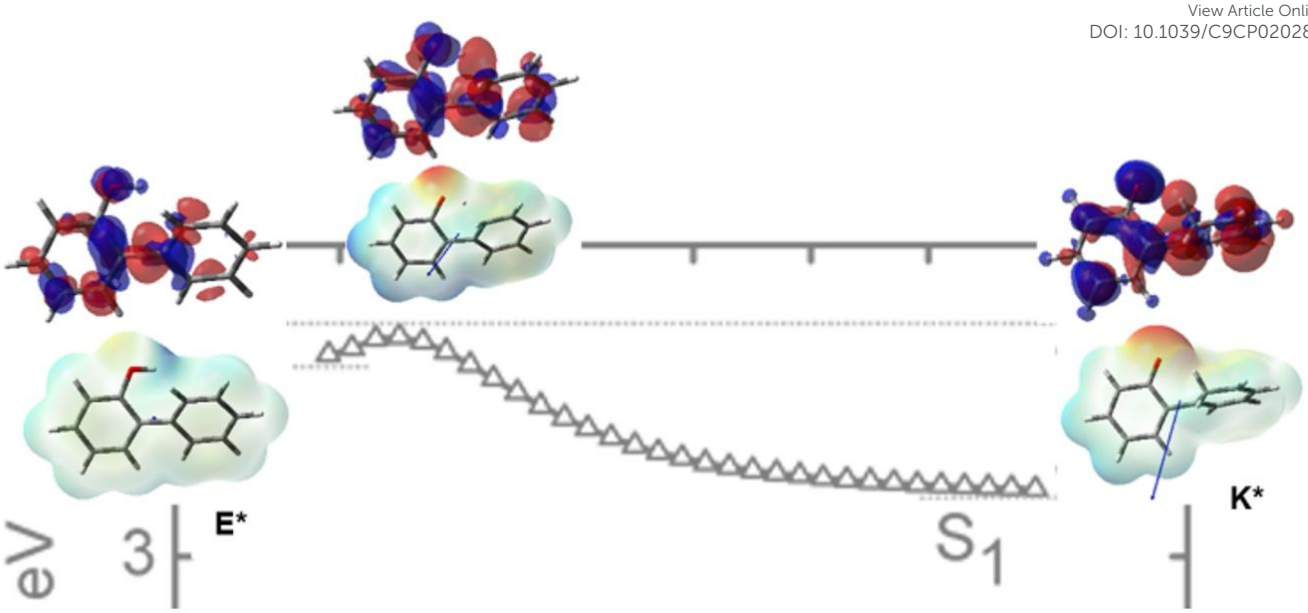

Fig. 4 Density difference plots (isovalue= 0.018 a.u.), ESP maps and dipole moment vectors at critical points (*enol* form, highest energy point and *keto* form) along the S_1 potential energy surface for **1**. E* and K* address for excited-state enol form and twisted keto tautomer, respectively.

singlet state, in agreement with the information collected from our theoretical IR frequencies analysis. According to the calculations, the O-H stretching vibrational frequency decreases from 3742 cm^{-1} in S_0 to 3625 cm^{-1} at the S_1 *enol* (E*) minimum, indicating a considerable OH···π interaction strengthening upon excitation. The same trend was found for derivatives **2** and **5**, as expected (see ESI 4.3.4).

Ground-state intramolecular proton transfer (GSIPT) exhibits an energy barrier of 1.8 eV, too large for allowing thermal PT. In S_1 state the ESIPT process is almost barrierless, leading to the *keto* form (K*) in a highly exergonic fashion. TD-DFT describes K* as a true minimum in the S_1 PES, but since at that geometry S_1 and S_0 are separated by 0.8 eV the probability of a $S_1 \rightarrow S_0$ non-radiative decay to occur is quite high. Indeed, Xia *et al*. reported the existence of a conical intersection (CI) in that region.[21a] The characterization of such critical point lies beyond the scope of the present work; nevertheless, it is worth to note that TD-DFT is capable of giving reasonable results despite its well-known breakdown in the neighbourhood of a CI.[23] No planar *keto* minimum was located in S_1 at TD-DFT level; actually, as the dihedral angle between rings gets closer to 0°, the potential energy surface does not exhibit a minimum, but rather the opposite (Fig. S4). We observed a twisting in the dihedral angle between rings occurring concomitantly with the proton translocation to the 2'-position of the phenyl ring in S_1. These geometry changes are in accordance with the increasing charge transfer character along the O-H coordinate (Fig. 4), as observed by Basaric *et al.* for 2-phenyl-1-naphthol at RI-CC2 level of theory.[21c] Once K* twisted form decays to S_0 the basal K* structure relaxes to planar K (dihedral angle between rings=0°) or *anti*-K (dihedral angle=180°) structures. It should be noted that the formation of a planar *ortho*-quinone methide does not take place in S_1, but rather occurs after relaxation to S_0. This torsional relaxation of *keto* tautomer to a twisted state was also previously described in other typical ESIPT systems as a decay channel competing with radiative transitions and leading to fluorescence quenching.[24] Unlike those systems, in which the excited *keto* form exists as a planar minimum in S_1 responsible for the characteristic Stokes-shifted ESIPT emission, 2-phenylphenol shows no proton-transfer emission, suggesting the absence of a planar *keto* tautomer stable enough to emit fluorescence, in accordance with the results presented herein. In general, the dipole moment change for the $S_1 \rightarrow S_0$ transition is very large; to explain the smaller dipole moment of K* with respect to the S_0 *keto* tautomer some authors suggested that twisted conformations in S_1 possess biradicaloid nature.[24a] A significant electron density redistribution is necessary to occur for the *enol*→*keto* tautomerization, making the phenyl ring basic enough to receive the incoming proton. Such electron density relocalization is absent in ground state, which explain the large energy barrier found. The change of electron density upon excitation can be seen on Figure 5. The most important feature is the gain of density of the phenyl ring (in red), which is connected with the stabilization of the *keto* tautomer.

For compounds having EWGs this density increase is lower, becoming almost negligible when R=CN. The installation of a

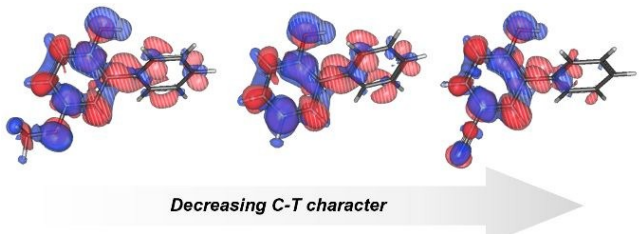

Fig. 5 Density difference plot (isovalue=0.0009 a.u.). The red/blue zones indicate an increase/decrease of the electronic density upon absorption of light for the $S_0 \rightarrow S_1$ transition of **2** (left), **1** (middle) and **5** (right).

View Article Online DOI: 10.1039/C9CP02038D

Table 6. Dipole moment magnitudes and long-range extent for compounds **1**, **2** and **5** in acetonitrile at CAM-B3LYP/6-31+G(d) level of theory.[a]

	Compounds		
	1 (H)	**2 (OMe)**	**5 (CN)**
S_0 μ E form (D)	2.4	4.7	7.0
S_1 μ E*form (D)	0.3	0.9	7.2
S_0 μ K form (D)	6.2	4.1	9.4
S_1 μ K* form (D)	5.3	7.6	1.7
Long-range extent Λ (a.u.)	0.698	0.624	0.705

[a] Molecular geometries and dipole moment vectors are shown in ESI 4.3.5

strong EWG in the molecule greatly affect the charge transfer process, diminishing the amount of electron density transferred to the phenyl ring. The long-range extent (Λ)[25] calculated by us through the computation of the overlap integral between the Slater coefficients of the main transitions contributing to vertical excitation for **1**, **2** and **5** revealed a reduction in the charge transfer degree as the electron withdrawing character of substituent rises (Table 6). Because of this effect, the **5** PES lies at higher energies than the others, making ESIPT slightly difficult (Fig. S3). Also, the K* form of **5** exhibits the greatest separation from S_0 (1.28 eV, Table 5) which could result in a less efficient passing through a conical intersection. Moreover, comparing the Merz-Kollman charges of E* with those of K*, it can be noted that a quite small amount of positive charge is transferred to phenyl ring when phototautomerization takes place. The phenol moiety charge varies from 0.071 q_e for E* to -0.163 q_e for *keto* tautomer, indicating that a charge of 0.234 (a 23.4% of a full proton) is transferred, whereas in ground state the phenol charge difference obtained is about 0.302 q_e. For **5**, this trend becomes greater: the difference in phenol charge is about 0.099 q_e (9% of proton) in S_1 and 0.446 q_e (44.6%) in ground state. According to these results, the studied photoprocess in S_1 can be catalogued as ESIHT (excited state intramolecular hydrogen transfer) rather than ESIPT, as Luber *et al.* proposed for a related system.[26] As a matter of fact, in a more strictly sense, the process should be described as an excited-state PCET (proton coupled electron transfer).[27] Together with our results on photoacidity, these findings strongly suggest that the attaching of an EWG in the phenol moiety of 2-phenylphenol decline ESIPT performance as result of a double effect, that is, intrinsic ESIPT partially hindering and improvement of adiabatic ESPT to bulk solvent, depleting the number of excited molecules able to experience ESIPT.

Unlike other systems in which the intramolecular proton transfer in S_1 occurs very efficiently (e.g. 2-phenyl-1-naphthol, with a D-exchange quantum yield of 0.73), ESIPT in 2-phenylphenol is a rather inefficient process, with a low reaction quantum yield (0.041). In this paper we have addressed adiabatic deprotonation as one of the causes contributing to the low ESIPT yield, but other factors (for example, the location of a conical intersection nearby the relaxed *enol* form in S_1 providing an additional non-radiative decay channel)[21a] must be considered. In previous works, the unfavourable conformational distribution in ground state has been pointed out as the most suitable explanation for the poor ESIPT performance of 2-phenylphenol. Basarić *et al.* showed that the *anti* conformer of **1** with one explicit water molecule (**1-W**, Fig. S14) in S_0 is more stable than the *syn* conformer by 1.46 kcal mol^{-1} at RI-CC2 level.[21c] Our calculations at DFT/B3LYP/6-31+G(d,p) level gave a similar energy difference in acetonitrile (1.16 kcal mol^{-1} for **1-W**), very close to the reported results obtained with the coupled cluster method. The energy difference between *syn* and *anti* conformers for **2-W** and **5-W** was 0.53 kcal mol^{-1} and 1.44 kcal mol^{-1}, respectively. The Boltzmann population of *syn* conformer in each case (29% for **2-W**, 12% for **1-W** and 8% for **5-W**) clearly indicates that the presence of an EWG in the molecule tips the balance in favor of the *anti* conformer. Therefore, unfavourable conformation in ground state constitute another factor contributing to the low ESIPT efficiency of the CN-derivative. Nevertheless, the prevalence of *anti* conformer in S_0 seems to be an intrinsic limitation of 2-phenylphenol system, certainly absent for 2-phenyl-1-naphthol since the 8-H avoids OH positioning away from phenyl moiety, making the *anti* isomer less stable. In order to overcome this limitation, we designed a new 2-phenylphenol derivative (**6**, Scheme 3) bearing bulky *t*-butyl groups at *ortho* and *para* position of phenol ring in order to minimize adiabatic deprotonation effects and to control conformer distribution. The photolysis of **6** in a 3:1 CH_3CN/D_2O mixture with 254 nm light yielded >99% of D-incorporation at the *ortho* position of the phenyl ring after 1 h. Mass spectra analysis agrees with ^{1}H NMR results, indicating the presence of dideuterated species as the major product (83%). Theoretical calculations at ground state in acetonitrile at B3LYP/6-31+G(d,p) level demonstrate that *syn* **6** conformer is indeed more stable than *anti* **6** by 3.0 kcal mol^{-1}, as expected. These results strongly support the previous theoretical approach and represent the first example of ESIPT to C-atom enhancement by using steric hindrance as a tool for controlling ground-state conformer distribution, and it also constitutes one of the few examples of ESIPT tuning via alkyl-substituent perturbation.[28]

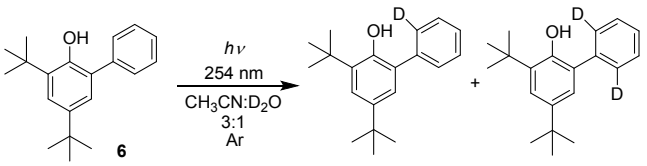

Scheme 3 Photochemical reaction of 3,5-di-*tert*-butyl-2-phenyphenol

Conclusions

In summary, the competition existing between excited-state proton transfer to bulk solvent and ESIPT was revealed by tuning the photoacidity of a series of 2-phenylphenols. The installation of an EWG in the molecule makes 2-phenylphenol a superphotoacid, favoring adiabatic deprotonation in excited state and thus hindering ESIPT. Additionally, the theoretical

View Article Online
DOI: 10.1039/C9CP02028D

calculations demonstrated that the EWGs also diminish the charge transfer character of vertical excitation to S_1 singlet state, which has a considerable impact on the basicity of C atoms of phenyl ring. Both facts combined provide evidence that the observed lost in efficiency is the result of -at least- two different factors related with ESPT to solvent and ESIPT intrinsic reactivity. Furthermore, unfavorable conformational distribution in ground state leading to a major population of *anti* isomer is another important cause of low ESIPT extent. This limitation was avoided by attaching bulky, EDG groups at the *ortho* and *para* positions of phenol ring, minimizing both *anti* form prevalence and adiabatic deprotonation. The remarkable ESIPT performance shown by such compound clearly demonstrates that, besides photoacidity, other factors must be considered to develop a better understanding of the process. Thus, the efficiency of ESIPT to C in a typical system can be improved through a careful molecular design. We expect our results to have a significant impact on the design of new similar ESIPT compounds with improved performances for future potential applications.

Experimental

Chemicals. All reagents (phenols, phenyl boronic acid, Pd-derived catalysts and bases) were obtained from Sigma-Aldrich and used as received. Solvents used for Suzuki-Miyaura reactions were also used as received. Acetonitrile for irradiation was dried, distilled and stored under molecular sieves (4 Å) and nitrogen atmosphere until its use. Deuterium oxide was donated by Central Nuclear Embalse (Córdoba, Argentina), and used as received.

Instrumentation. Gas chromatographic analysis was performed on a Varian GC with a flame ionization detector, and equipped with a VF-5 ms, 30 m x 0.25 mm × 0.25 mm column. ^{1}H NMR, ^{13}C NMR and 2D NMR were recorded on a 400 MHz Bruker nuclear magnetic resonance spectrometer. Fluorescence spectra of the samples dissolved in the described solvent were recorded with an Agilent Cary Eclipse Fluorescence Spectrophotometer. Time-resolved fluorescence measures were taken with a Deltaflex Horiba Spectrofluorometer using a diode laser (λ = 267 nm) for the excitation of the samples. UV-visible spectra of the compounds in solution were recorded with a Shimadzu UV-1800 Spectrophotometer. HRMS were recorded on a Bruker, MicroTOF Q II equipment, operated with an ESI source in (positive/negative) mode, using nitrogen as nebulizing and drying gas and sodium formiate 10 mM as internal standard. Gas Chromatographic/Mass Spectrometer analysis were carried out on a Shimadzu GC–MS QP 5050 spectrometer equipped with a VF-5 ms, 30 m × 0.25 mm × 0.25 mm column.

Steady-state photolysis. Solutions of acetonitrile:deuterium oxide (3:1) containing p-substituted phenylphenols 1-5 (ca. 2.20 mM) were irradiated under argon atmosphere (irradiation time = 1 h). The irradiation source was a Luzchem multilamp photoreactor ORG-model containing 10 low-pressure Hg lamps (max= 254 nm). After this time, the acetonitrile was evaporated under reduced pressure and the leftover was extracted employing CH_2Cl_2 and water. The organic layer was dried over $MgSO_4$ and evaporated under reduced pressure. The dry crude was analyzed by NMR and CG-MS. NMR spectra and MS results are described in ESI.

Computational details. All DFT and TD-DFT calculations were performed the Gaussian 09 package.[29] The relevant stationary points were fully optimized by using the range-separated correction of B3LYP functional, CAM (Coulomb Attenuating Method)[30] with the 6-31+G(d) basis set. The obtained stationary points were characterized by Hessian diagonalization and harmonic frequency analyses to obtain zero-point and thermal corrections for the energies, enthalpies and free energies. Solvation effects were simulated with PCM model, using the dielectric constant of acetonitrile. Relaxed scans were computed by allowing all the internal degrees of freedom to relax apart from the driving coordinate (O-H distance, step length=0.05 Å). Vertical excitation and emission energies were calculated within the LR-PCM (linear response) scheme. For the determination of pK_a values the B3LYP/6-311+G(d,p)/SMD level of theory was employed in water. To calculate pK_a* values, the vertical absorption and emission energies for undeprotonated species were simulated using the CAM-B3LYP functional with the 6-31+G(d) basis set. The absorption and emission energies of deprotonated species were computed at the same level of theory. The corresponding wavelengths are informed in Table S2; some values were refined using the non-equilibrium state specific correction[31] in order to gain deeper accuracy. For NCI analysis the Multiwfn software was employed.[32] For the calculation of the long-range extent, Λ was defined as usual:[25]

$$\Lambda = \frac{\sum_{i,a} \kappa_{ia}^2 \int |\varphi_i(r)||\varphi_a(r)|\, dr}{\sum_{i,a} \kappa_{ia}^2}$$

where κ_{ia} are the coefficients of each contributing $\phi_i \rightarrow \phi_a$ orbital transition, with $0 < \Lambda < 1$ (Λ =1 for a totally local transition; smaller values signifies increasing charge transfer character); the integrals were computed using Gabedit 2.4.8 and the cubman facility of Gaussian09.[33] Visualization and graphics rendering were carried out with GaussView 5.0.8,[34] Gabedit 2.4.8 and VMD 1.9.3.[35] The electronic energies in Hartrees, zero-point energies and thermal corrections are available in Table S5, as well as the whole set of Cartesian coordinates for all the stationary points (SI 4.4).

Synthesis and characterization of compounds 1-6.

[1,1'-Biphenyl]-2-ol (2-Phenylphenol) (1).[36] 2-Iodo-phenol (1 equiv, 1 mmol) and phenylboronic acid (1 equiv, 1 mmol) were added to a Schlenk tube with 10 mL of distilled water. Then, K_2CO_3 (4 equiv, 4 mmol) and Pd/C (2% mol, 21 mg) were added to the mixture and stirred. The system was heated to 80 °C for 16 h. For the extraction process diethyl ether (3 x 10 mL) and acidified water were used. The organic extract was dried with Na_2SO_4, filtered, and evaporated under reduced pressure. Products were first identified by GC and GC–MS. The compound was isolated from the crude by column chromatography as a colorless oil, employing a mixture of

pentane/CH_2Cl_2 (90:10) as eluent. The product was obtained with 40% yield, 70 mg. ^{1}H NMR (400 MHz, $(CD_3)_2CO$, 25 ºC): δ= 8.27 (s, 1H, OH); 7.59 (d, ^1J(H,H)= 7.9 Hz, 2H); 7.39 (t, ^1J(H,H)= 7.9 Hz, 2H); 7.31-7.28 (m, 2H); 7.18 (dt, ^1J(H,H)= 8.1 Hz, ^2J(H,H)= 1.4 Hz, 1H); 6.99 (d, ^1J(H,H)= 8.1 Hz, 1H); 6.93 (t, ^1J(H,H)= 7.6 Hz, 1H). MS (EI): m/z: 170 (100%), 169 (74%), 141 (39%), 115 (33%), 63 (6%).

5-Methoxy-[1,1'-biphenyl]-2-ol (2).[37] It was followed the procedure described by Camargo Solórzano *et al*. with slightly modifications.[38] 2-Bromo-4-methoxyphenol (1 equiv, 0.67 mmol) and phenylboronic acid (1.3 equiv, 0.9 mmol) were added to a Schlenk tube with a 5 mL of dioxane:water (4:1) under inert atmosphere (N_2). Then, $K_3PO_4.H_2O$ (3 equiv, 2 mmol), PPh_3 (10% mol) and $Pd(dba)_2$ (5% mol, 19 mg) were added to the mixture and stirred by 24 hs at 90 ºC. For the extraction process diethyl ether (3 x 10 mL) and acidified water were used. The organic extract was dried with Mg_2SO_4, filtered, and evaporated under reduced pressure. Products were first identified by GC and GC−MS. The compound was isolated from the crude by column chromatography (hexane/CH_2Cl_2 at 9.5:0.5 ratio) followed by a preparative TLC with hexane/CH_2Cl_2 (8:2) as eluent. The product was obtained as a pale brown oil, 18% yield, 24 mg. ^{1}H NMR (400 MHz, $(CD_3)_2CO$, 25 ºC): δ= 7.83 (s, 1H, OH); 7.60 (d, ^1J(H,H)= 7.7 Hz, 2H); 7.39 (t, ^1J(H,H)= 7.8 Hz, 2H); 7.29 (t, ^1J(H,H)= 7.5 Hz, 1H); 6.91 (d, ^1J(H,H)= 8.7 Hz, 1H); 6.86 (ds, ^2J(H,H)= 3.0 Hz, 1H); 6.77 (dd, ^1J(H,H)= 8.7 Hz, ^2J(H,H)= 3.0 Hz, 1H); 3.77 (s, 3H, CH_3). MS (EI): *m/z*: 200 (100%), 185 (83%), 157 (34%), 128 (34%), 129 (18%), 115 (10%), 102 (8%), 77 (8%).

5-(tert-Butyl)-[1,1'-biphenyl]-2-ol (3).[39] It was followed the procedure described by Camargo Solórzano et *al*. with slightly modifications.[38] 2-bromo-4-(*tert*-butyl)phenol (1 equiv, 0.5 mmol) and phenylboronic acid (1.1 equiv, 0.55 mmol) were added to a Schlenk tube with 5 mL of distilled water. Then, $(n\text{-}Bu)_4N^+Br^-$ (3% equiv), CsF (4 equiv, 2 mmol) and Pd/C (2% mol, 10 mg) were added to the mixture. The system was heated to 80 °C and stirred by 2.5 h. For the extraction process diethyl ether (3 x 10 mL) and acidified water were used. The organic extract was dried with Na_2SO_4, filtered, and evaporated under reduced pressure. Products were first identified by GC and GC−MS. The compound was isolated from the crude by column chromatography as pale yellow oil, employing a linear gradient of eluent composed by pentane and CH_2Cl_2, from a ratio 90:10 ratio to 70:30. The product was obtained with 36% yield, 41 mg. ^{1}H NMR (400 MHz, $(CD_3)_2CO$, 25 ºC): δ= 8.06 (s, 1H, OH); 7.59 (d, ^1J(H,H)= 7.8 Hz, 2H); 7.40 (t, ^1J(H,H)= 7.8 Hz, 2H); 7.32-7.27 (m, 2H); 7.23 (dd, ^1J(H,H)= 8.5 Hz, ^2J(H,H)= 2.2 Hz, 1H); 6.91 (d, ^1J(H,H)= 8.5 Hz, 1H); 1.32 (s, 9H, 3xCH_3). MS (EI): *m/z*: 226 (24%), 211 (100%), 183 (12%), 165 (8%), 152 (8%), 91 (21%).

6-Hydroxy-[1,1'-biphenyl]-3-carboxylic acid and Methyl 6-hydroxy-[1,1'-biphenyl]-3-carboxylate (4).[40] 3-Bromo-4-hydroxybenzoic acid (1 eq, 1.16 mmol), phenylboronic acid (1.16 mmol, 1 eq.), palladium(II)acetate (0.035 mmol, 0.03 eq.) and 1.5M cesium carbonate (aqueous) (2.3 mL) were dissolved in DMF (5 mL) at room temperature under nitrogen then heated at 45° C for 24 hours. Worked up by adding water (10 mL) then adjusting to pH=3 with 1N HCl. Extracted the acidic aqueous 3 times with ethyl acetate. The ethyl acetate layers were combined and rinsed 3 times with water (10 mL). The ethyl acetate layer was then dried over Na_2SO_4 and then, the solvent was evaporated under reduced pressure. The oil was purified over silica gel in 1:1 hexanes/ethyl acetate. The product was obtained as oil, 50% yield. A third part of this acid was used for the photolysis at 254 nm in CH_3CN/D_2O. ^{1}H NMR (400 MHz, $(CD_3)_2CO$, 25 ºC): δ= 9.24 (s, 1H, OH); 8.00 (ds, ^2J(H,H)= 2.2 Hz, 1H); 7.90 (dd, ^1J(H,H)= 8.4 Hz, ^2J(H,H)= 2.2 Hz, 1H); 7.62 (d, ^1J(H,H)= 8.5 Hz, 2H); 7.44 (t, ^1J(H,H)= 7.7 Hz, 2H); 7.34 (t, ^1J(H,H)= 7.6 Hz, 1H); 7.09 (d, ^1J(H,H)= 8.5 Hz, 1H). When $(CD_3)_2SO$ is used as solvent, the signal of the proton for the COOH group is detected at δ 12.47 ppm. MS (EI): *m/z*: 214 (100%), 197 (34%), 169 (18%), 141 (28%), 115 (24%), 98 (10%). The rest was dissolved in 10 mL of methanol and put in a round bottom flask, then, 50 µL of concentrated H_2SO_4 was added. The reaction was refluxed overnight. The crude was purified over silica gel using an eluent gradient (pentane/ethyl acetate) starting from 100 % of pentane. The product was obtained as white solid, 50% yield, 44 mg. ^{1}H NMR (400 MHz, $(CD_3)_2CO$) δ= 9.26 (s, 1H, OH); 7.965 (ds, ^2J(H,H)= 2.3 Hz, 1H); 7.86 (dd, ^1J(H,H)= 8.4 Hz, ^2J(H,H)= 2.3 Hz, 1H); 7.61-7.59 (m, 2H); 7.44 (t, ^1J(H,H)= 7.4 Hz, 2H); 7.34 (t, ^1J(H,H)= 7.4 Hz, 1H); 7.08 (d, ^1J(H,H)= 8.4 Hz, 1H); 3.85 (s, 3H, CH_3). ^{13}C NMR (100 MHz, $(CD_3)_2CO$) δ= 167.1 (q, C=O); 159.5 (q, C_{Ar}-OH); 138.7 (q, C_{Ar}); 133.2 (C_{Ar}-H); 131.1 (C_{Ar}-H); 130.1 (2 C_{Ar}-H); 129.4 (q, C_{Ar}); 128.9 (2 C_{Ar}-H); 128.0 (C_{Ar}-H); 122.9 (q, C_{Ar}); 116.9 (C_{Ar}-H); 51.9 (CH_3). MS (EI): *m/z*: 228 (61%), 197 (100%), 141 (21%), 115 (22%), 98 (21%), 70 (16%). HRMS (ESI-TOF) m/z $[M + Na]^+$ Calcd for $C_{14}H_{12}O_3Na$: 251.0679; Found: 251.0660.

6-Hydroxy-[1,1'-biphenyl]-3-carbonitrile (5).[41] It was followed the procedure described by Zhao *et* al. et *al*. with slightly modifications.[41] 2-Bromo-4-methoxyphenol (1 equiv, 0.67 mmol) and phenylboronic acid (1.3 equiv, 0.9 mmol) were added to a Schlenk tube with a 5 mL of dioxane:water (4:1) under inert atmosphere (N_2). Then, $K_3PO_4.H_2O$ (3 equiv, 2 mmol), PPh_3 (10% mol) and $Pd(dba)_2$ (5% mol, 19 mg) were added to the mixture and stirred by 24 hs at 90 ºC. For the extraction process diethyl ether (3 x 10 mL) and acidified water were used. The organic extract was dried with Mg_2SO_4, filtered, and evaporated under reduced pressure. Products were first identified by GC and GC−MS. The compound was isolated from the crude by column chromatography (hexane/CH_2Cl_2 at 9.5:0.5 ratio) followed by a preparative TLC with hexane/CH_2Cl_2 (8:2) as eluent. The product was obtained as pale brown oil, 18% yield, 24 mg. ^{1}H NMR (400 MHz, $(CD_3)_2CO$, 25 ºC): δ= 9.51 (s, 1H, OH); 7.675 (ds, ^2J(H,H)= 1.9 Hz, 1H); 7.62-7.58 (m, 3H); 7.44 (t, ^1J(H,H)= 7.3 Hz, 2H); 7.37 (t, ^1J(H,H)= 7.3 Hz, 1H); 7.16 (d, ^1J(H,H)= 8.4 Hz, 1H). MS (EI): *m/z*: 195 (100%), 194 (82%), 167 (13%), 166 (25%), 140 (20%), 139 (16%), 115 (6%), 84 (8%).

3,5-di-tert-butyl-[1,1'-biphenyl]-2-ol (6). 2,4-di-*tert*-Butylphenol (1 equiv, 1 mmol) and phenylboronic acid (1.2 equiv, 0.55 mmol) were added to a Schlenk tube with 5 mL of distilled water. Then, $(n\text{-}Bu)_4N^+Br^-$ (3% equiv), CsF (4 equiv, 4 mmol) and Pd/C (2% mol, 20 mg) were added to the mixture. The procedure followed is the same one used for the synthesis of compound **3**, until to obtain the pure compound. The product was obtained with 16% yield, 44 mg. ^{1}H NMR (400 MHz, $(CD_3)_2CO$, 25 ºC): δ= 7.45 (d, *J*(H,H)= 4.4 Hz, 4H); 7.37-7.33 (m, 2H); 7.06 (ds, ^2J(H,H)= 2.4 Hz, 1H); 6.69 (s,1H, OH); 1.47 (s, 9H, 3 CH_3); 1.32 (s, 9H, 3 CH_3). ^{13}C NMR (100 MHz, $(CD_3)_2CO$) δ= 150.3 (q, C_{Ar}-OH); 142.6 (q, C_{Ar}); 139.8 (q, C_{Ar}); 136.9 (q, C_{Ar}); 130.5 (2 C_{Ar}-H); 130.1 (q, C_{Ar}); 129.7 (2 C_{Ar}-H); 128.1 (C_{Ar}-H); 125.8 (C_{Ar}-H); 123.9 (C_{Ar}-H); 35.8 (q, CCH3); 34.8 (q, CCH3); 31.9 (3 CH_3); 30.2 (3 CH_3). HRMS (ESI-TOF) m/z $[M + Na]^+$ Calcd for $C_{20}H_{26}ONa$: 305.1876; Found: 305.1867.

View Article Online
DOI: 10.1039/C9CP02028D

Conflicts of interest

There are no conflicts to declare.

Acknowledgements

This work was partly supported by the Consejo Nacional de Investigaciones Científicas y Técnicas (CONICET), Secretaría de Ciencia y Tecnología, Universidad Nacional de Córdoba (SECyT), and the Agencia Nacional de Promoción Científica y Técnica (ANPCyT). L. D. Mena gratefully acknowledges a fellowship from CONICET.

References

1 (a) V. Balzani, P. Ceroni, A. Juris, in *Photochemistry and Photophysics. Concepts, Research, Applications*, Wiley-VCH, Verlag GmbH & Co. KGaA, Weinheim, 2014, ch. 4; (b) D. Pines and E. Pines, in *Handbook of Hydrogen Transfer, e*d. R. L. Schowen, WILEY-VCH Verlag GmbH & Co. KGaA, Weinheim, 2006, ch. 12; (c) J. F. Ireland, P. A. H. Wyatt, *Adv. Phys. Org. Chem.,* 1976, **12**, 131-221.
2 K. M. Solntsev, D. Huppert, N. Agmon, L. M. Tolbert, *J. Phys. Chem. A.,* 2000, **104**, 4658-4669.
3 (a) S. Kaneko, S. Yotoriyama, H. Koda, S. Tobita, *J. Phys. Chem. A.,* 2009, **113**, 3021-3028; (b) D. Huppert, L. M. Tolbert, S. Linares-Samaniego, *J. Phys. Chem. A,* 1997, **101**, 4602-4605; (c) N. Agmon, D. Huppert, A. Masad, E. Pines, *J. Phys. Chem.,* 1991, **95**, 10407-10413.
4 S. P. Webb, L. A. Philips, S. W. Yeh, L. M. Tolbert, J. H. Clark, *J. Phys. Chem.,* 1986, **90**, 5154-5164.
5 Y. Liao, *Acc. Chem. Res.,* 2017, **50**, 1956-1964.
6 P. Zhou, K. Han, *Acc. Chem. Res.,* 2018, **51**, 1681-1690.
7 G. W. Robinson, *J. Phys. Chem.,* 1991, **95**, 10386-10391.
8 (a) D. Maus, A. Grandjean, G. Jung, *J. Phys. Chem. A.,* 2018, **122**, 9025-9030; (b) O. Gajst, L. P. d. Silva, J. C. G. E. d. Silva, D. Huppert, *J. Phys. Chem. A.,* 2018, **122**, 6166-6175; (c) B. Finkler, C. Spies, M. Vester, F. Walte, K. Omlor, I. Riemann, M. Zimmer, F. Stracke, M. Gerhards, G. Jung, *Photochem. Photobiol. Sci.,* 2014, **13**, 548-552; (d) C. Spies, B. Finkler, N. Acarb, G. Jung, *Phys. Chem. Chem. Phys.,* 2013, **15**, 19893-19905.
9 T. Kumpulainen, B. Lang, A. Rosspeintner, E. Vauthey, *Chem. Rev.,* 2017, **117**, 10826-10939.
10 R. Pollard, S. Wu, G. Zhang, P. Wan, *J. Org. Chem.,* 1993, **58**, 2605-2613.
11 M. Lukeman, in *Quinone Methides*, ed. S. E. Rokita, John Wiley & Sons, Inc., Hoboken, 2009, ch. 1.
12 V. S. Padalkar, S. Seki, *Chem. Soc. Rev.,* 2016, **45**, 169-202.
13 M. Lukeman, P. Wan, *Chemical Communications,* 2001, **0**, 1004-1005.
14 (a) Y.-H. Wang, P. Wan, *Photochem. Photobiol. Sci.,* 2013, **12**, 1571-1588; (b) Y.-H. Wang, P. Wan, *Photochem. Photobiol. Sci.,* 2011, **10**, 1934-1944; (c) M. Lukeman, M.-D. Burns, P. Wan, *Can. J. Chem.,* 2011, **89**, 433-440; (d) N. Basarić, P. Wan, *Photochem. Photobiol. Sci.,* 2006, **5**, 656-664.
15 (a) C. Azarias, S. Budzak, A. D. Laurent, G. Ulrich, D. Jacquemin, *Chem. Sci.,* 2016, **7**, 3763-3774; (b) H. W. Tseng, J. Q. Liu, J. A. Chen, C. M. Chao, K. M. Liu, C. L. Chen, T. C. Lin, C. H. Hung, Y. L. Chou, T. C. Lin, T.-L. Wang, P.-T. Chou, *J. Phys. Chem. Lett.,* 2015, **6**, 1477-1486; (c) A. J. Stasyuk, M. K. Cyrański, D. T. Gryko, M. Solà, *J. Chem. Theory Comput.,* 2015, **11**, 1046-1054.
16 M. Lukeman, P. Wan, *J. Am. Chem. Soc.,* 2002, **124**, 9458-9464.
17 The discrepancy between our result and the previously published 55% value may be due to imponderable experimental details; however, the obtained result is a valid reference control for all subsequent measurements.
18 G. Granucci, J. T. Hynes, P. Millié, T.-H. Tran-Thi, *J. Am. Chem. Soc.,* 2000, **122**, 12243-12253.
19 (a) A. Weller, *Prog. React. Kinet.,* 1961, **1**, 187; (b) T. Förster, *Z. Elektrochem.,* 1950, **54**, 531.
20 (a) J. Jover, R. Bosque, J. Sales, *QSAR Comb. Sci.,* 2007, **26**, 385-397; (b) A. Albert, E. P. Serjeant, *The Determination of Ionization Constants. A Laboratory Manual.*, 3rd ed., Chapman and Hall, New York, 1984.
21 (a) S.-H. Xia, B.-B. Xie, Q. Fang, G. Cui, W. Thiel, *Phys. Chem. Chem. Phys.,* 2015, **17**, 9687-9697; (b) N. Basarić, N. Došlić, J. Ivković, Y. H. Wang, J. Veljković, K. Mlinarić-Majerski, P. Wan, *J. Org. Chem.,* 2013, **78**, 1811-1823; (c) N. Basarić, N. Došlić, J. Ivković, Y.-H. Wang, M. Mališ, P. Wan, *Chem. Eur. J.,* 2012, **18**, 10617-10624.
22 C. Schriever, M. Barbatti, K. Stock, A. J. A. Aquino, D. Tunega, S. Lochbrunner, E. Riedle, R. d. Vivie-Riedle, H. Lischka, *Chem. Phys.,* 2008, **347**, 446-461.
23 B. G. Levine, C. Ko, J. Quenneville, T. J. Martinez, *Mol. Phys.,* 2006, **104**, 1039-1051.
24 (a) F. A. S. Chipem, G. Krishnamoorthy, *J. Phys. Chem. A,* 2009, **113**, 12063-12070; (b) M. Barbatti, A. J. A. Aquino, H. Lischka, C. Schriever, S. Lochbrunner, E. Riedle, *Phys. Chem. Chem. Phys.,* 2009, **11**, 1406-1415; (c) D. LeGourriérec, V. Kharlanov, R. G. Brown, W. Rettig, *J. Photochem. Photobiol. A,* 2000, **130**, 101-111.
25 M. J. G. Peach, P. Benfield, T. Helgaker, D. J. Tozer, *J. Chem. Phys.,* 2008, **128**, 044118: 1-8.
26 S. Luber, K. Adamczyk, E. T. J. Nibbering, V. S. Batista, *J. Phys. Chem. A,* 2013, **117**, 5269-5279.
27 C.-C. Hsieh, C.-M. Jiang, P.-T. Chou, *Acc. Chem. Res.,* 2010, **43**, 1364-1374.
28 Z.-Y. Liu, J.-W. Hu, C.-L. Chen, Y.-A. Chen, K.-Y. Chen, P.-T. Chou, *J. Phys. Chem. C.,* 2018, **122**, 21833-21840.
29 M. J. Frisch, G. W. Trucks, H. B. Schlegel, G. E. Scuseria, M. A. Robb, J. R. Cheeseman, G. Scalmani, V. Barone, B. Mennucci, G. A. Petersson, H. Nakatsuji, M. Caricato, X. Li, H. P. Hratchian, A. F. Izmaylov, J. Bloino, G. Zheng, J. L. Sonnenberg, M. Hada, M. Ehara, K. Toyota, R. Fukuda, J. Hasegawa, M. Ishida, T. Nakajima, Y. Honda, O. Kitao, H. Nakai, T. Vreven, J. A. Montgomery Jr., J. E. Peralta, F. Ogliaro, M. Bearpark, J. J. Heyd, E. Brothers, K. N. Kudin, V. N. Staroverov, R. Kobayashi, J. Normand, K. Raghavachari, A. Rendell, J. C. Burant, S. S. Iyengar, J. Tomasi, M. Cossi, N. Rega, J. M. Millam, M. Klene, J. E. Knox, J. B. Cross, V. Bakken, C. Adamo, J. Jaramillo, R. Gomperts, R. E. Stratmann, O. Yazyev, A. J. Austin, R. Cammi, C. Pomelli, J. W. Ochterski, R. L. Martin, K. Morokuma, V. G. Zakrzewski, G. A. Voth, P. Salvador, J. J. Dannenberg, S. Dapprich, A. D. Daniels, Ö. Farkas, J. B. Foresman, J. V. Ortiz, J. Cioslowski, D. J. Fox, Gaussian 09, Revision E.01, Gaussian, Inc., Wallingford CT, 2009.
30 T. Yanai, D. P. Tew, N. C. Handy, *Chem. Phys. Lett.,* 2004, **393**, 51-57.
31 R. Improta, G. Scalmani, M. J. Frisch, V. Barone, *J. Chem. Phys.,* 2007, **127**, 074504: 1-9.
32 T. Lu, F. Chen, *J. Comput. Chem.,* 2012, **33**, 580-592.
33 A.-R. Allouche, *J. Comput. Chem.,* 2011, **32**, 174-182.
34 GaussView, Version 5, Roy Dennington, Todd Keith, and John Millam, Semichem Inc., Shawnee, Mission, KS, 2009.
35 Visual Molecular Dynamics (VMD), version 1.8.9, http://www.ks.uiuc.edu/Research/vmd.

View Article Online
DOI: 10.1039/C9CP02028D

36 B. Xiao, T. J. Gong, Z. J. Liu, J. H. Liu, D. F. Luo, J. Xu, L. Liu, *J. Am. Chem. Soc.,* 2011, **133**, 9250-9253.
37 (a) N. Haga, H. Takayanagi, *J. Org. Chem.,* 1996, **61**, 735-745; (b) R. Beugelmans, M. Bois-Choussy, *Tetrahedron Lett.,* 1988, **29**, 1289-1292.
38 P. C. Solórzano, F. Brigante, A. B. Pierini, L. B. Jimenez, *J. Org. Chem.,* 2018, **83**, 7867-7877.
39 B. Xiao, Y. Fu, J. Xu, T.-J. Gong, J.-J. Dai, J. Yi, L. Liu, *J. Am. Chem. Soc.,* 2010, **132**, 468-470.
40 P. H. Carter, R. J. Cherney, D. G. Batt, J. V. Duncia, D. S. Gardner, S. S. Ko, A. S. Srivastava, M. G. Yang*, Vol. 7,829,571 B2*, US, 2010, p. 147.
41 J. Zhao, Y. Wang, Y. He, L. Liu, Q. Zhu, *Org. Lett.,* 2012, **14**, 1078-1081.